Comparative Medicine
Copyright 2007
by the American Association for Laboratory Animal Science

Vol 57, No 5
October 2007
Pages 450–459

Mice Transgenic for Human Angiotensin-converting Enzyme 2 Provide a Model for SARS Coronavirus Infection

Xiu-hong Yang,[1] Wei Deng,[1] Zan Tong,[2] Yan-xia Liu,[2] Lian-feng Zhang,[1] Hua Zhu,[1] Hong Gao,[1] Lan Huang,[1] Ya-li Liu,[1] Chun-mei Ma,[1] Yan-feng Xu,[1] Ming-xiao Ding,[2] Hong-kui Deng,[2,*] and Chuan Qin[1,*]

To establish a small animal model of severe acute respiratory syndrome (SARS), we developed a mouse model of human severe acute respiratory syndrome coronavirus (SARS-CoV) infection by introducing the human gene for angiotensin-converting enzyme 2 (hACE2) (the cellular receptor of SARS-CoV), driven by the mouse *ACE2* promoter, into the mouse genome. The *hACE2* gene was expressed in lung, heart, kidney, and intestine. We also evaluated the responses of wild-type and transgenic mice to SARS-CoV inoculation. At days 3 and 7 postinoculation, SARS-CoV replicated more efficiently in the lungs of transgenic mice than in those of wild-type mice. In addition, transgenic mice had more severe pulmonary lesions, including interstitial hyperemia and hemorrhage, monocytic and lymphocytic infiltration, protein exudation, and alveolar epithelial cell proliferation and desquamation. Other pathologic changes, including vasculitis, degeneration, and necrosis, were found in the extrapulmonary organs of transgenic mice, and viral antigen was found in brain. Therefore, transgenic mice were more susceptible to SARS-CoV than were wild-type mice, and susceptibility was associated with severe pathologic changes that resembled human SARS infection. These mice will be valuable for testing potential vaccine and antiviral drug therapies and for furthering our understanding of SARS pathogenesis.

Abbreviations: hACE2, human angiotensin-converting enzyme 2; IFA, immunofluorescent assay; RT-PCR, reverse transcription–polymerase chain reaction; SARS-CoV, SARS coronavirus; $TCID_{50}$, 50% tissue culture infectious dose

Severe acute respiratory syndrome coronavirus (SARS-CoV) was identified as the etiologic agent of SARS,[10,11,15,17,22] which was first isolated in South China in November 2002 and spread rapidly through many countries.[4,30,39] SARS infection is accompanied by respiratory symptoms, high fever, headache, and myalgia, followed by acute respiratory distress and respiratory failure.[2,33,38] The fatality rate is approximately 10%.[7] Autopsy studies reported diffuse alveolar damage as the most prominent feature in patients who succumbed to SARS infection;[13,18] one study also reported systemic vasculitis and toxicity in 3 patients who died of the disease.[6] Although the spread of SARS was controlled rapidly through traditional quarantine and sanitation measures, the molecular mechanism of infection remains unclear, and SARS-CoV could reemerge in the human population at any time.

Animal models provide an important tool for studying SARS pathogenesis and evaluating the efficacy of potential drugs and vaccines. Established models for SARS infection include cynomologus macaques, ferrets, cats, mice, African green monkeys, and Golden Syrian hamsters.[3,11,19,23,26–29] Nonhuman primate models using intratracheal inoculation appear to mimic the clinical features and lung pathologic changes of human SARS infection most accurately, whereas current rodent models are associated with mild lung inflammation and rapid viral clearance. Taking ethical issues, cost, and maintenance into account, we aimed to establish a more susceptible SARS rodent model that could be used for the development of specific antiviral drugs and vaccines.

The spike proteins of SARS-CoV bind to receptors on host cells and mediate viral entry.[1,31,36] The metallopeptidase angiotensin-converting enzyme 2 (ACE2) was identified as a functional receptor for SARS-CoV, indicating that a mouse transgenic for human *ACE2* (*hACE2*) could serve as an animal model for SARS infection.[20,21,35] Recent studies show that SARS-CoV infection is lethal in *hACE2* transgenic mice.[24,34] These mice express *hACE2* under regulation of a global promoter or cytokeratin 18 promoter in many organs and show rapid weight loss after intranasal inoculation, which rapidly develops into a lethal infection. In this report, we describe a new *hACE2* transgenic mouse model for SARS coronavirus. We describe the method by which the *hACE2* gene was introduced into the mouse genome, a more limited tissue distribution of hACE2 expression, and the permissiveness of *hACE2* transgenic mice to SARS-CoV infection, thus more closely mimicking the human condition.

Materials and Methods

Production of transgenic mice. *hACE2* cDNA was cloned as previously described[35] and inserted into the pEGFP-N1 plasmid (BD Biosciences) upstream of the SV40 polyA tract, replacing the coding sequence for enhanced green fluorescence protein. We retrieved the mouse *ACE2* promoter (9 kilobases) by digesting bacterial artificial chromosome (RP23-75P20) DNA with *Kpn*I and *Eco*RV and inserted it upstream of the *hACE2* coding sequences (Figure 1).

Received: 14 Mar 2007. Revision requested: 16 Apr 2007. Accepted: 24 Apr 2007.
[1]Institute of Laboratory Animal Science, Chinese Academy of Medical Sciences (CAMS) and Peking Union Medical College (PUMC), Beijing, PR China; [2]Department of Cell Biology and Genetics, College of Life Sciences, Peking University, Beijing, PR China
[*]Corresponding authors. Email: qinchuan@pumc.edu.cn; hongkui_deng@pku.edu.cn

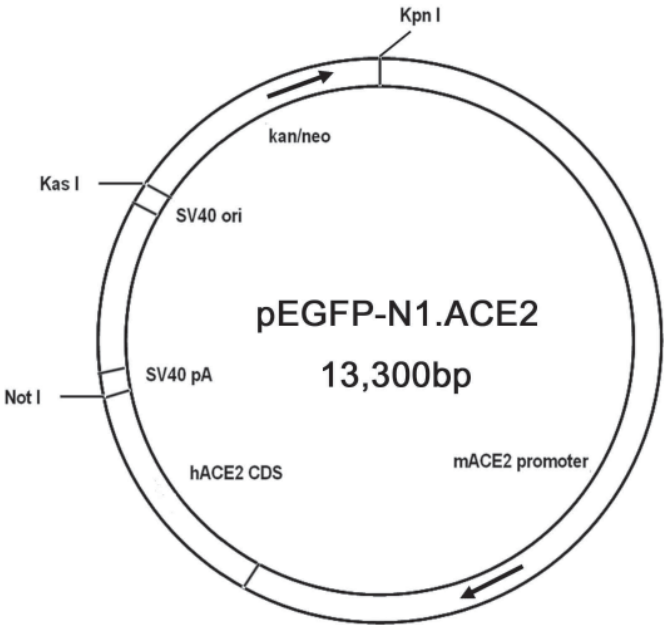

Figure 1. Construction of the hACE2 transgene. The coding sequence (CDS) for enhanced green fluorescence protein in pEGFP-N1 was replaced by the hACE2 coding sequence, and the mouse ACE2 promoter was inserted upstream of the hACE2 cDNA.

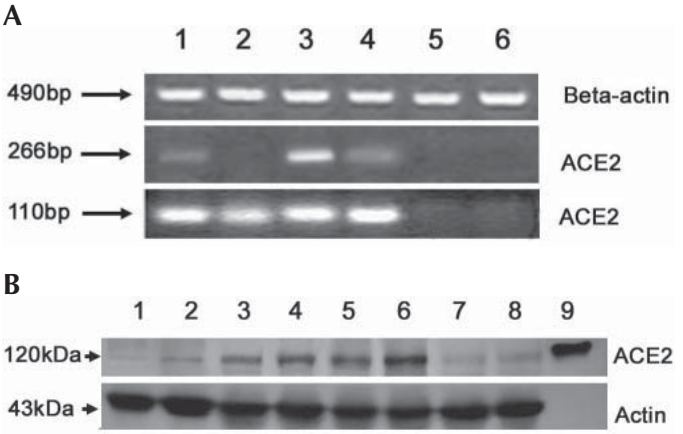

Figure 2. Analysis of hACE2 expression in transgenic mice. (A) The upper panel shows expression of mouse β actin (the internal control). The middle panel shows expression of hACE2 by using RT-PCR, and the lower panel shows expression of hACE2 by nested PCR. Lanes 1 through 6 represent lung, heart, kidney, intestine, liver, and spleen, respectively. (B) The upper panel shows hACE2 protein expression by Western blot. The lower panel shows β actin as an internal control. Lanes 1, 3, 5, and 7 represent lung, heart, kidney, and intestine of wild-type mice, whereas lanes 2, 4, 6, and 8 represent lung, heart, kidney, and intestine of transgenic mice. Lane 9 represents recombinant hACE2 protein used as a positive control.

After *hACE2* was identified in transfected NIH3T3 cells, the plasmid was linearized with *Kpn*I and *Kas*I and purified with phenol. Fragments carrying the mouse *ACE2* promoter driving the *hACE2* coding sequence were introduced by microinjection into the pronuclei of fertilized ova from ICR mice. The injected zygotes then were transplanted into the oviducts of pseudopregnant mice. Mice in which the transgene integrated were identified from tail biopsies. These mice were bred to produce offspring for analysis.

Polymerase chain reaction (PCR) amplification. PCR amplification was used to screen for the transgene in the genomic DNA of potential transgenic mice. One pair of primers designed to detect *hACE2* by PCR (sense, 5′ ATG TCA AGC TCT TCC TGG CTC CTT CTC AGC 3′; antisense, 5′ GCA AGT GTG GAC TGT TCC TT 3′) corresponded to nucleotide positions 1 through 30 and 219 through 239 of *hACE2* cDNA, whereas the other (sense, 5′ TTG AGC CCT TAT TTA CCT 3′; antisense, 5′ TTT CAA ATT AGC CAC TCG 3′) corresponded to positions 1763 through 1780 and 2011 through 2028. The amplification parameters used were: 5 min at 94 °C; 30 cycles of 30 s at 94 °C, 30 s at 60 °C (first pair of primers) or 50 °C (second pair), and 30 s at 72 °C; and a final extension of 10 min at 72 °C.

Reverse transcription–PCR (RT-PCR) and nested RT-PCR assays. To detect *hACE2* mRNA expression in the tissues of transgenic mice, 2 μg total RNA that had been treated with DNase I (New England Biolabs, Ipswich, MA) to eliminate DNA contaminants was converted to cDNA by using a DT primer (Promega, Madison, WI) and amplified using the primers 5′ TTG AGC CCT TAT TTA CCT 3′ and 5′ TTT CAA ATT AGC CAC TCG 3′ for the initial PCR followed by the internal primers 5′ TTG AGC CCT TAT TTA CCT 3′ and 5′ ATA TGG ACT CCA GTC GGT AC 3′, which were used for the nested PCR.

To test for SARS-CoV in mouse lungs on days 3 and 7 postinoculation, total RNA was extracted from homogenized lung tissue by using Trizol reagent (Invitrogen, Carlsbad, CA). Reverse transcription was performed in a 20-μl volume containing 1 μg template RNA. SARS-CoV was amplified by PCR using the following primers: sense, 5′ ATG AAT TAC CAA GTC AAT GGT TAC 3′; antisense, 5′ CAT AAC CAG TCG GTA CAG CTA C 3′. The amplification parameters used were: 1 h at 42 °C for reverse transcription; 5 min at 94 °C; 28 cycles of 30 s at 94 °C, 30 s at 55 °C, and 30 s at 72 °C; and final extension for 10 min at 72 °C. As a control, β actin was amplified by using the following primers: sense, 5′ GTC GTA CCA CAG GCA TTG TGA TGG 3′; antisense, 5′ GCA ATG CCT GGG TAC ATG GTG G 3′. Amplification parameters were identical to those just described.

Western blot. The Mem-PER Eukaryotic Membrane Protein Extraction Reagent Kit (Pierce, Rockford, IL) was used to extract membrane proteins from the tissues, according to the manufacturer's protocol. For Western blot analysis, nitrocellulose (Amersham, Piscataway, NJ) was incubated with monoclonal anti-hACE2 ectodomain antibody (1:200; R&D Systems, Minneapolis, MN) followed by incubation with a peroxidase-conjugated secondary antibody (1:50,000; Santa Cruz Biotechnology, Santa Cruz, CA). Bound antibodies were visualized by chemoluminescence (Amersham). To control for the amount of protein loaded in each lane, β actin was used as an internal standard.

Animal infection studies. The female ICR mice used in this experiment were hemizygous for the transgene. After approval for animal experiments was obtained from the institutional animal welfare committee, mice were handled in a Biosafety Level 3 laboratory at our institute. Transgenic mice (age, 6 mo) were maintained under specific-pathogen-free husbandry conditions and acclimated to the Biosafety Level 3 laboratory prior to inoculation. Sex-, age-, and background-matched wild-type mice were used as controls. Each mouse was inoculated intranasally with 10^5 of the 50% tissue culture infective dose of SARS-CoV strain PUMC01 (GenBank accession no., AY350750) in 40 μl normal saline. Sham-inoculated mice received normal saline. On days 3

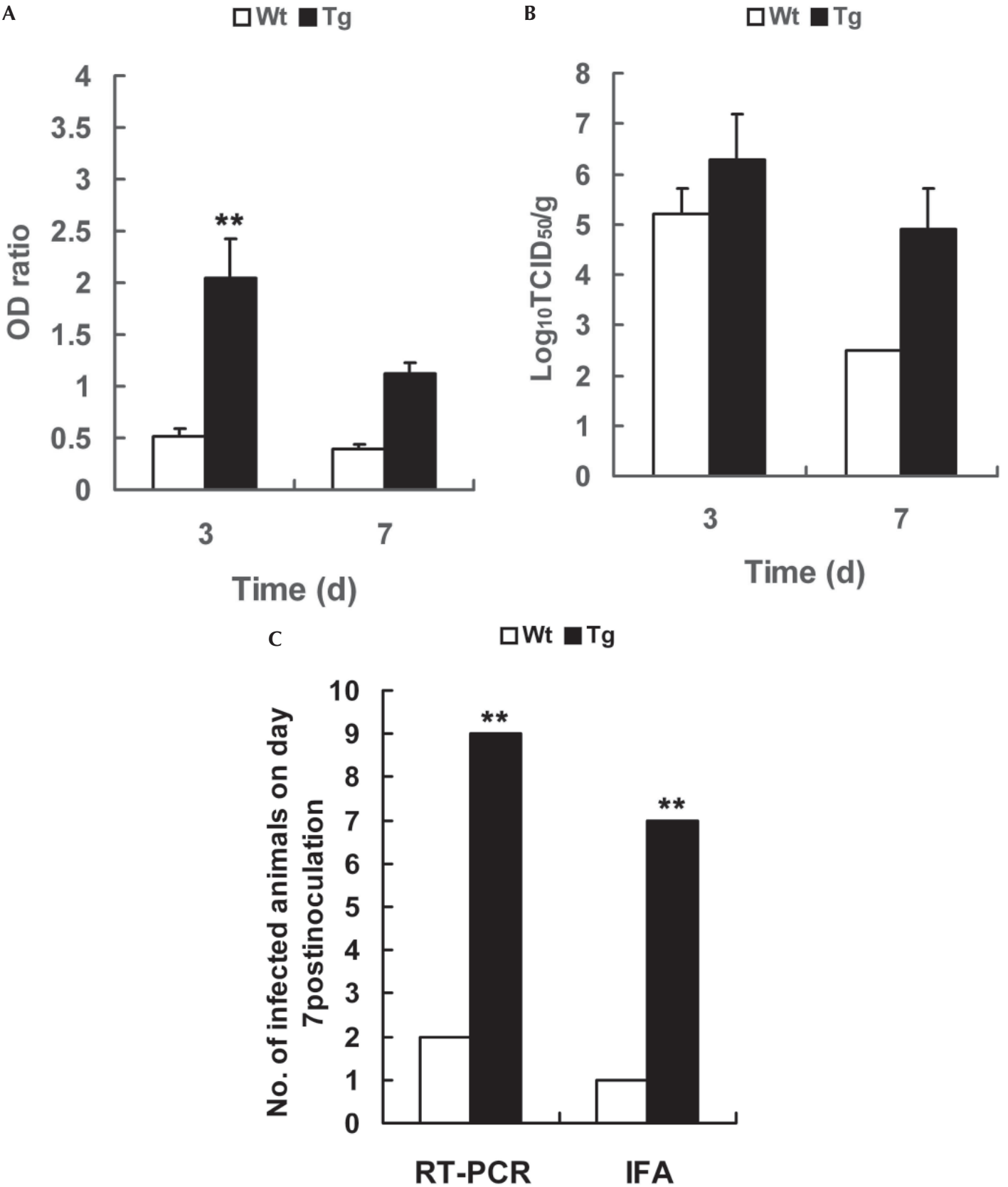

Figure 3. Semiquantitative analysis of infected transgenic and wild-type mice by RT-PCR and IFA. (A) Semiquantitative analysis by RT-PCR. (B) Viral titers of homogenated lung supernatants. (C) Numbers of infected animals in the transgenic and wild-type groups on day 7 postinoculation. OD, optical density; Tg, transgenic mice; Wt, wild-type mice; n = 7 on day 3, and n = 9 on day 7; **, $P < 0.01$ versus the wild-type group.

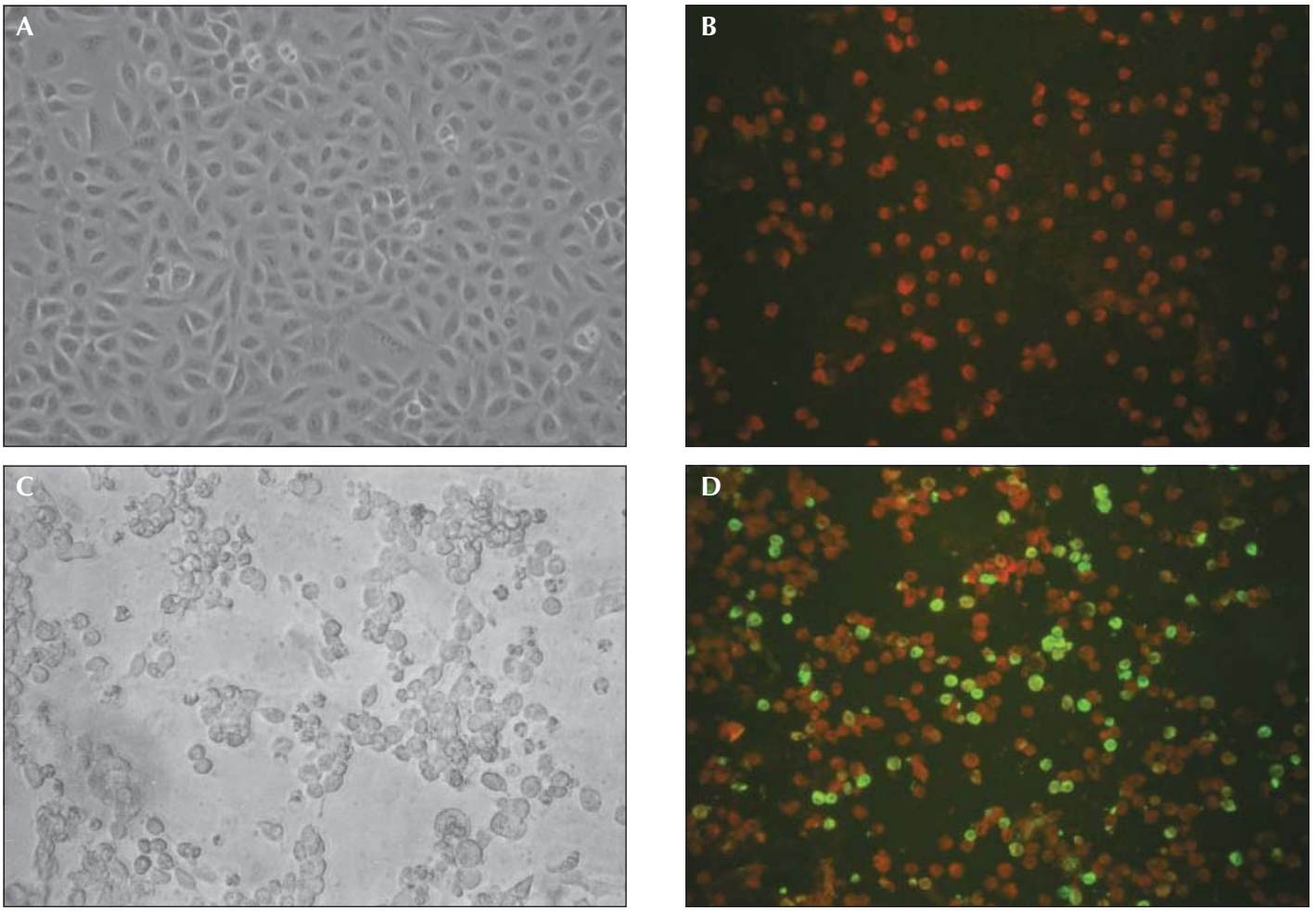

Figure 4. Cytopathic effect caused by SARS-CoV, and IFA for SARS-CoV S protein. (A) Monolayer of normal uninfected Vero E6 cells. (B) SARS-CoV-uninfected VeroE6 cells show a negative signal for cytoplasmic SARS-CoV S protein (red fluorescence). (C) VeroE6 cell monolayers infected by SARS-CoV show a viral cytopathic effect. (D) SARS-CoV-infected VeroE6 cells show a positive signal for SARS-CoV S protein in the cytoplasm (green fluorescence). Magnification, ×200.

and 7 postinoculation, 9 mice in each group were euthanized and tissue samples harvested. The left lungs were fixed in neutral buffered formalin, and the right lungs were stored at –70 °C.

Isolation of SARS-CoV and immunofluorescent assay (IFA). SARS-CoV was isolated from the supernatants of lung homogenates, as previously described.[19] The infection status of tested animals was determined by cytopathic effect and IFA. Anti-SARS S protein monoclonal antibody (1:200, Starvax, Beijing, China) was incubated with prepared slides for 40 min at 37 °C. After rinsing with phosphate-buffered saline, the fluoroscein isothiocyanate-labeled secondary antibody (Zymed, San Francisco, CA), diluted with phosphate-buffered saline containing 0.02% Evans Blue (Sigma, St Louis, MO), was incubated with the slides for 20 min at 37 °C. Viral titers in supernatants from lung homogenates were expressed as the number of $TCID_{50}$ per gram of tissue.

Histopathology and immunohistochemistry. Harvested organs were processed for routine hematoxylin and eosin staining. Immunohistochemical staining was used to detect SARS-CoV antigens as described previously.[19] In brief, sections were deparaffinized, rehydrated, and subjected to heat-induced antigen retrieval by incubation in citrate buffer (pH 6.0). Endogenous peroxidase was blocked with 3% H_2O_2 in methanol. Anti-SARS S protein monoclonal antibody (1:200, Starvax), a gift from Dr Yiyou Chen, was inoculated for 2 h at 37 °C. Antibody binding was detected with polyperoxidase-conjugated goat anti-rabbit immunoglobulin G (Zymed). Peroxidase activity was developed by using 3, 3′-diaminobenzidine tetrachloride (Zymed). Counterstaining was performed by using hematoxylin. For negative control tests, sections were inoculated with phosphate-buffered saline in the absence of primary antibodies.

Image analysis and statistical analysis. Results of SARS-CoV RT-PCR and hACE2 Western blot were expressed as ratios of the summed intensity values of the target bands to those of internal controls by using UVIPhoto and UVISoft (UVIBand Application, version 97.04, Topac, Cohasset, MA). Viral titer results were expressed as the mean ± 1 standard deviation. Results were analyzed by *t* test by using SPSS 11.0 software (SPSS, Chicago, IL). The proportions of SARS-CoV infection in the wild-type and transgenic groups were compared by chi-square test by using SAS 9.1 software (SAS Institute, Cary, NC).

Results

Production of *hACE2* transgenic mice. *hACE2* was detected in

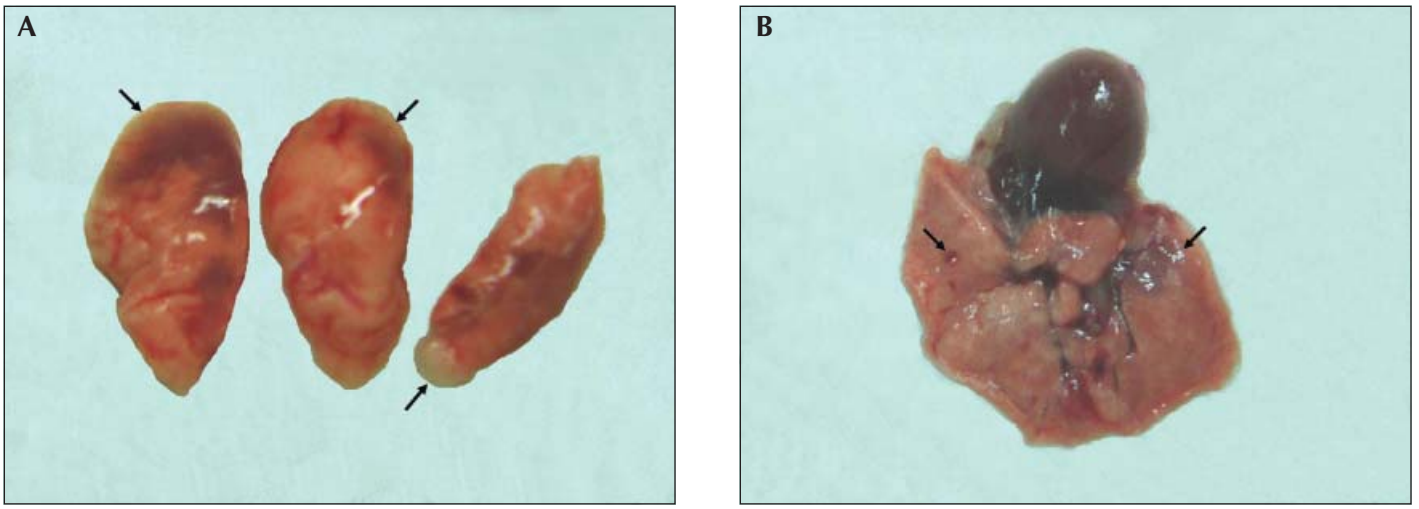

Figure 5. Gross lung specimens from 2 representative transgenic mice challenged with SARS-CoV that were obtained on (A) day 3 and (B) day 7 postinfection. Local lesions are indicated by arrows.

the tail biopsies of 4 animals. Nucleotide sequences of the PCR products were 100% identical to those of *hACE2* mRNA (GenBank accession no., NM 021804). Transgenic mice were mated with wild-type ICR mice, and the transgene was maintained in a hemizygous state. The transmission rate of the *hACE2* gene was approximately 50% for all transgenic mouse lines. Hemizygous animals had no evidence of negative effects, such as sudden death, due to transgene insertion.

Expression of *hACE2* in mice. Among the tested tissues (lung, heart, kidney, intestine, liver, and spleen), *hACE2* mRNA was detected by RT-PCR in the lung, kidney, and intestine of F1 offspring from 1 of the 4 founders. We went on to characterize this founder line as a model of human SARS infection. To analyze expression of the human gene in other organs in the transgenic mice, we designed another pair of primers and performed nested PCR. These results revealed that *hACE2* mRNA could also be detected in the heart of this *hACE2* founder line (Figure 2 A). RNA analysis showed that *hACE2* mRNA was transcribed in the lung, heart, kidney, and intestine of transgenic mice.

Transgenic mice assessed by Western blot expressed higher levels of recombinant hACE2 protein with the expected molecular size (120 kDa) in the expected 4 tissues than did wild-type mice (Figure 2 B). The mean intensities of hACE2 protein were expressed as the ratio of the optical density of the hACE2 protein band to that of β actin. hACE2 protein levels in tested tissues from 3 transgenic mice were all more than 30% higher than those in the 3 wild-type mice. The hACE2 protein was most highly expressed in the kidneys of transgenic mice.

Susceptibility to SARS-CoV. None of 36 challenged wild-type and transgenic mice was dead by 1 wk postinfection, but 8 transgenic mice became lethargic. To confirm whether the challenged mice were infected, we tested the lung tissues of mice by using IFA and RT-PCR in parallel. The results indicated that the same numbers of transgenic and wild-type mice were infected by day 3 postinoculation. However, Both the mean optical density ratio of nucleic acid of SARS-CoV to β actin and the mean viral titer of the lung homogenates of transgenic mice were higher than those of wild-type mice (Figure 3 A, B).

By day 7 after postinoculation, only 1 of 9 wild-type mice was positive by viral isolation, with a titer of less than $10^{2.5}$ $TCID_{50}$/g. In contrast, 7 of 9 transgenic mice showed viral titers ($10^{4.9\pm0.8}$ $TCID_{50}$/g) at this time point (Figure 3 B, C). These data indicate that viral infection was clearing in both groups but was clearing more rapidly in the wild-type animals. Vero E6 cells challenged with homogenates from uninfected lung tissue did not show any cytopathic effect (Figure 4 A) and displayed a negative IFA signal (red color, Figure 4 B), whereas those challenged with infected lung homogenates demonstrated a cytopathic effect (Figure 4 C) and a positive IFA signal (green color) for SARS-CoV (Figure 4D).

Pathologic changes. Transgenic mice showed more severe pathologic changes, both anatomically and histologically, than did wild-type mice. Five transgenic mice had gross pulmonary edema, focal hemorrhage, consolidation, and lung bullae (Figure 5 A, B), whereas wild-type mice had no visible changes. Uninfected challenged transgenic mice had not any pathologic changes (Figure 6 A). Infected wild-type mice had mild interstitial pneumonia at day 3 postinfection (Figure 6 B). In contrast, infected transgenic mice had more severe pulmonary damage accompanied by interstitial hyperemia, edema, inflammatory cell infiltration (including both monocytes and lymphocytes), markedly thickened interstitia, broken alveolar walls, extensive consolidation, compensatory emphysema (Figure 6 C), and extensive hemorrhage. Some blood vessels had become degenerated and were surrounded by monocytic and lymphocytic infiltrates (Figure 6 D). Type II alveolar cells had undergone marked proliferation and formed multinucleated pneumocytes. Desquamative pulmonary alveolitis and bronchitis were also present, as well as multinucleated macrophages in the alveoli (Figure 6 D). Pathologic changes in the lungs of mice were more severe on day 3 than on day 7 postinfection.

We found extrapulmonary organ damage in 10 transgenic mice. Glomerular capillaries were dilated markedly and engorged, an obvious lymphocytic infiltrate was present in the renal interstitia, and proximal tubule epithelial cells revealed signs of degeneration (Figure 7 A). Pyelitis was observed in transgenic mice (Figure 7 B). Brain damage included ependymitis (Figure 7 C), vasculitis (Figure 7 D), and hemorrhage (Figure 7 E). Mild lymphocytic infiltration and sarcolemmal proliferation were present in cardiac interstitial tissue (Figure 7 F), and a lymphocytic infiltrate was

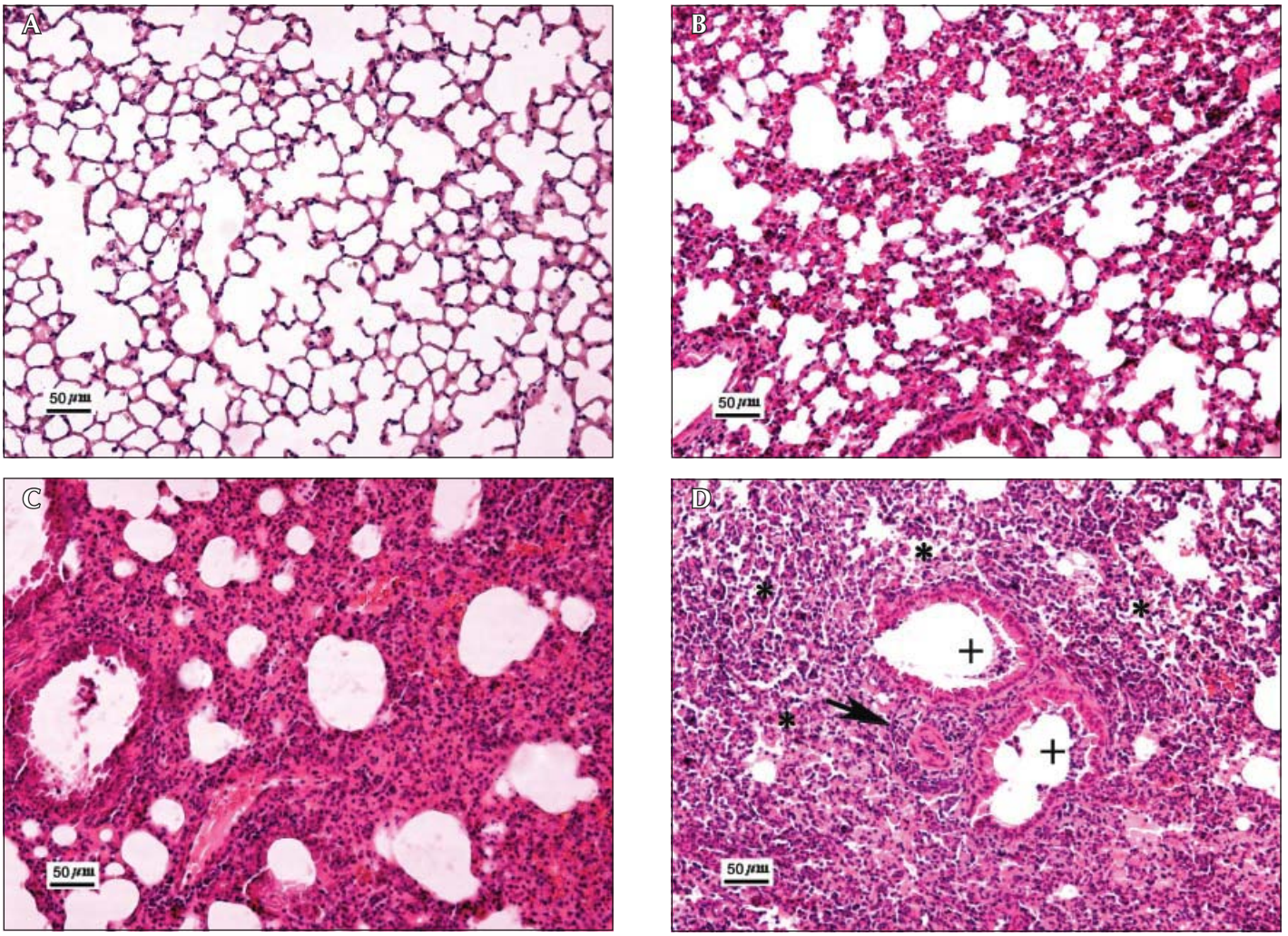

Figure 6. Pathologic changes in the lungs. (A) Lung of unchallenged transgenic mouse. (B) Lung of SARS-CoV-challenged wild-type mouse. (C) Inflammatory cell infiltrates, type II alveolar cell proliferation, markedly widened alveolar walls, and compensatory emphysema. (D) Desquamative pulmonary alveolitis (asterisks) and bronchitis (crosses), and monocyte and lymphocyte infiltration around the blood vessels (arrows). Hematoxylin and eosin stain; magnification, ×100; bar, 50 μm.

observed in the submandibular gland (Figure 7 G). Patchy necrosis was present in the liver (Figure 7 H). The mucosal layers of the stomach and small intestine showed signs of edema, small vessel dilation, and lymphocyte infiltration. Some epithelial cells in the small intestine were desquamative (Figure 7 I), and some lymph nodes showed severe hemorrhage and necrosis (Figure 7 J).

Tissue distribution of SARS-CoV. We used immunohistochemical techniques to detect SARS-CoV in the tissues of infected wild-type and transgenic mice. SARS-CoV was found in the vascular endothelial cells and epithelial cells of the alveoli of infected transgenic mice (Figure 8 A). However, no virus antigen was found in infected wild-type mice and unchallenged transgenic mice (Figure 8 B). Positive signals were also detected in the cerebral neurocytes (Figure 8 C) of severely infected transgenic mice. The kidney, heart, liver, stomach, and other organs of all infected mice were free of viral antigen (data not shown).

Discussion

The development of animal models to study SARS biology and pathogenesis is of interest to the scientific community, particularly if the models appropriately mimic human infection. Current SARS animal models, including ferrets, aged BALB/c mice, and genetically modified mice, have shown some clinical diseases and mortality.[23,27] In comparison, *hACE2* transgenic mice recently were shown to have 100% mortality. ACE2 is present in many human tissues, including the vascular endothelial cells of many organs, and the epithelial cells of the lung, small intestine, and kidney.[8,12] The transgenic animal model we describe in this study had hACE2 protein in lung, heart, kidney, and intestine; production of hACE2 was under control of the endogenous mouse ACE2 gene promoter. This expression pattern more closely mimicked native ACE2 distribution than that seen in 2 recent studies using *hACE2* transgenic mice in which hACE2 was under control of a cytokeratine promoter or a composite promoter consisting of a cytomegalovirus IE enhancer and the chicken actin promoter.[24,34] Although the physiologic function of the ACE2 molecule remains unknown, some studies have shown that ACE2 is essential for cardiac function and blood pressure maintenance.[5,8,25,32,37] Soluble

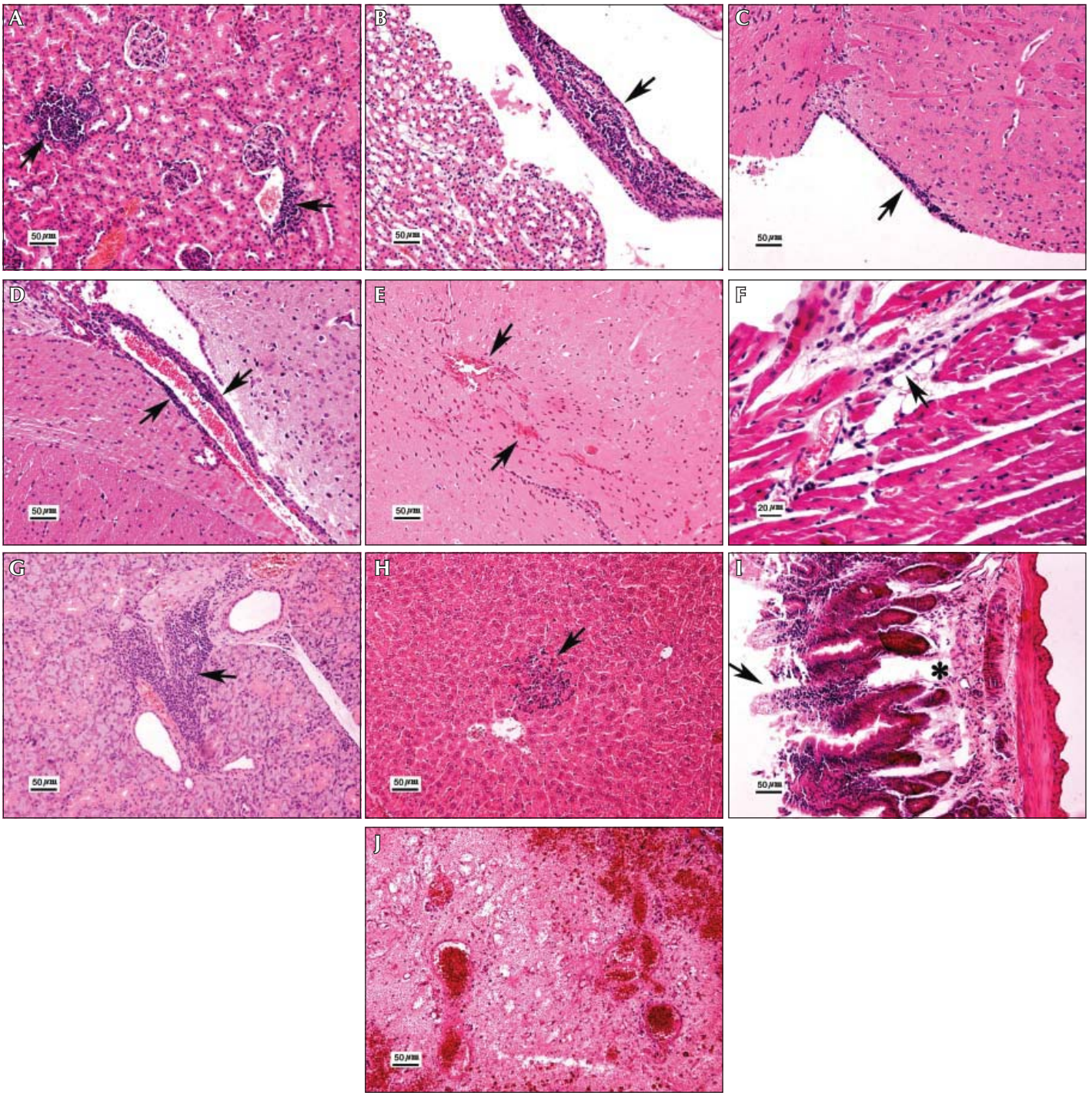

Figure 7. Pathologic changes in extrapulmonary organs of transgenic mice. (A) Infiltration of lymphocytes in the renal interstitium (arrows). (B) Pyelitis (arrow). (C) Ependymitis (arrow). (D) Cerebral vasculitis (arrows). (E) Cerebral hemorrhage (arrows). (F) Lymphocyte infiltration in the heart and sarcolemma proliferation in the cardiac interstitium (arrow). (G) Submaxillaritis (arrow). (H) Patchy necrosis in the liver (arrow). (I) Edema in the mucosal layer (asterisk) and epithelial cell desquamation (arrow) of the small intestine. (J) Hemorrhage and necrosis in the lymph nodes. Hematoxylin and eosin stain. Magnification, ×100 (A, B, C, D, E, G, H, I, J), ×200 (F); bar, 50 μm (A, B, C, D, E, G, H, I, J), 20 μm (F).

ACE2 protects mice from severe acute lung failure induced by SARS-CoV infection and the SARS-CoV spike protein.[14,16] Some researchers have shown that transgenic mice with elevated cardiac ACE2 expression levels had a higher incidence of sudden death.[9] None of our transgenic mice died suddenly, perhaps because of lower hACE2 expression in the heart.

Our results showed that transgenic mice had more severe pathologic changes in the lung tissue than did wild-type mice. Transgenic mice also manifested a systemic toxic reaction, prolonged viral persistence, and viral antigen in the cerebrum. Tissue

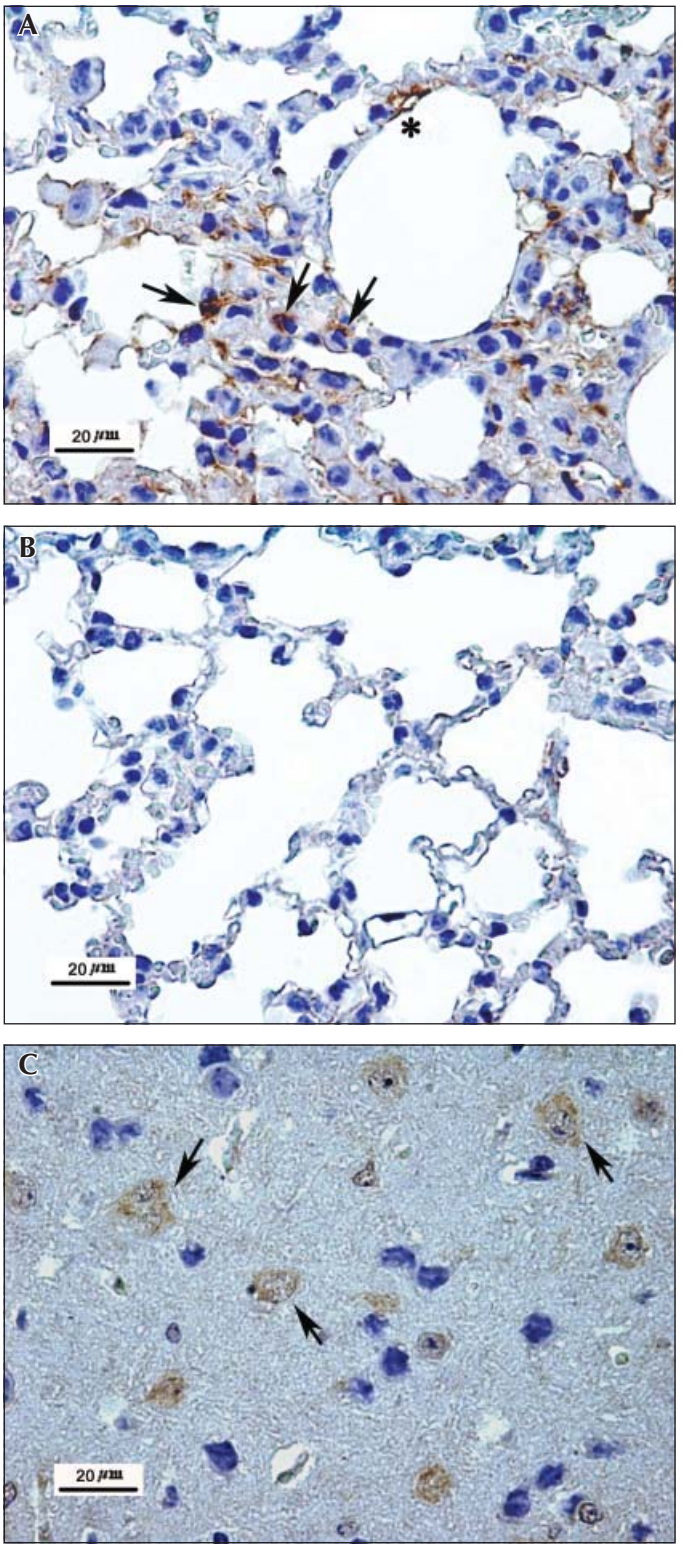

Figure 8. Tissue distribution of SARS-CoV by immunohistochemistry. (A) Viral antigen in epithelial cells (arrows) and vascular endothelial cells (asterisk) of the lung (brown cells). (B) No viral antigen in unchallenged transgenic mouse. (C) Viral antigen in the cerebral neurocytes (arrows, brown cells). Immunohistochemical stain and hematoxylin counterstain; magnification, ×400; bar, 20 μm.

distribution of the hACE2 protein, viral replication, and pathologic changes in the transgenic mice were similar to those in humans. These findings support validity of this SARS mouse model, despite the absence of mortality in transgenic mice when infected with SARS-CoV.

In contrast to 2 recent studies showing lethal SARS-CoV infection in *hACE2* transgenic mice with no evidence of diffuse alveolar damage,[24,34] none of the infected mice in our study died. This result may be due to the slightly lower dosage of virus was used or the lower level of hACE2 expression in transgenic mice. In comparison, the death rate of SARS in 2003 was about 10% and sometimes as high as 50% in people older than 60 y. The main pathologic change in SARS patients was diffuse alveolar damage. Our nonlethal model presented not only severe and typical interstitial pneumonia but also diverse and widespread extrapulmonary organ damage, which was very similar to that in some SARS patients.[6,13,18] These findings are very important for the potential application of the model for drug evaluation.

In the present study, transgenic mice with severe lung damage showed systemic inflammatory reactions, degeneration, and necrosis in many extrapulmonary organs; these types of damage may be induced directly or indirectly by severe SARS-CoV infection. Viral antigen was not detected in organs with marked pathologic change, such as the kidney, heart, and intestine, where hACE2 protein was expressed. The findings were consistent with notion that hACE2 was not the only receptor for SARS-CoV. The entry of SARS-CoV into host cells may require coreceptors. Perhaps hACE2 molecules on the cell surface of these tissues were able to bind SARS-CoV but lacked the ability to induce conformational changes required for entry. Other factors including microenvironment (for example, pH, ion concentrations) and mechanisms to support transcription and replication of the viral genome also may contribute to the permissiveness of SARS-CoV. The pathogenesis of SARS-CoV in our *hACE2* transgenic mice will require further study.

In summary, the *hACE2* transgenic mice described in this report were more susceptible to SARS-CoV than were wild-type mice, and their disease more closely mimicked the pathology of human SARS. Although it has the limitations of limited tissue distribution, decreased *hACE2* expression, and lack of lethality, this model likely still will facilitate the evaluation of anti-SARS-CoV drugs and vaccines and the analysis of SARS pathogenesis by virus detection and systemic pathologic studies.

Acknowledgments

We thank Qiang Wei, Hao Yu, and Linlin Bao for their technical assistance in virus isolation. We are indebted to Yaozeng Lu, Fang Yang, Guosheng Li, and Yunxin Chen for their technical assistance with pathology images and to Qi Kong for help in submitting this paper.

References

1. **Babcock GJ, Esshaki DJ, Thomas WD Jr, Ambrosino DM.** 2004. Amino acids 270 to 510 of the severe acute respiratory syndrome coronavirus spike protein are required for interaction with receptor. J Virol **78:**4552–4560.
2. **Booth CM, Matukas LM, Tomlinson GA, Rachlis AR, Rose DB, Dwosh HA, Walmsley SL, Mazzulli T, Avendano M, Derkach P, Ephtimios IE, Kitai I, Mederski BD, Shadowitz SB, Gold WL, Hawryluck LA, Rea E, Chenkin JS, Cescon DW, Poutanen SM, Detsky AS.** 2003. Clinical features and short-term outcomes of 144 patients with SARS in the greater Toronto area. JAMA **289:**2801–2809.

3. **Bukreyev A, Lamirande EW, Buchholz UJ, Vogel LN, Elkins WR, St Claire M, Murphy BR, Subbarao K, Collins PL.** 2004. Mucosal immunisation of African green monkeys (*Cercopithecus aethiops*) with an attenuated parainfluenza virus expressing the SARS coronavirus spike protein for the prevention of SARS. Lancet **363:**2122–2127.
4. **Centers for Disease Control and Prevention.** 2003. Update: outbreak of severe acute respiratory syndrome-worldwide, 2003. MMWR Morbid Mortal Wkly Rep **52:**241–248.
5. **Crackower MA, Sarao R, Oudit GY, Yagil C, Kozieradzki I, Scanga SE, Oliveira-dos-Santos AJ, da Costa J, Zhang L, Pei Y, Scholey J, Ferrario CM, Manoukian AS, Chappell MC, Backx PH, Yagil Y, Penninger JM.** 2002. Angiotensin-converting enzyme 2 is an essential regulator of heart function. Nature **417:**822–828.
6. **Ding Y, Wang H, Shen H, Li Z, Geng J, Han H, Cai J, Li X, Kang W, Weng D, Lu Y, Wu D, He L, Yao K.** 2003. The clinical pathology of severe acute respiratory syndrome (SARS): a report from China. J Pathol **200:**282–289.
7. **Donnelly CA, Ghani AC, Leung GM, Hedley AJ, Fraser C, Riley S, Abu-Raddad LJ, Ho LM, Thach TQ, Chau P, Chan KP, Lam TH, Tse LY, Tsang T, Liu SH, Kong JH, Lau EM, Ferguson NM, Anderson RM.** 2003. Epidemiological determinants of spread of causal agent of severe acute respiratory syndrome in Hong Kong. Lancet **361:**1761–1766.
8. **Donoghue M, Hsieh F, Baronas E, Godbout K, Gosselin M, Stagliano N, Donovan M, Woolf B, Robison K, Jeyaseelan R, Breitbart RE, Acton S.** 2000. A novel angiotensin-converting enzyme-related carboxypeptidase (ACE2) converts angiotensin I to angiotensin 1–9. Circ Res **87:**E1–E9.
9. **Donoghue M, Wakimoto H, Maguire CT, Acton S, Hales P, Stagliano N, Fairchild-Huntress V, Xu J, Lorenz JN, Kadambi V, Berul CI, Breitbart RE.** 2003. Heart block, ventricular tachycardia, and sudden death in ACE2 transgenic mice with downregulated connexins. J Mol Cell Cardiol **35:**1043–1053.
10. **Drosten C, Gunther S, Preiser W, van der Werf S, Brodt HR, Becker S, Rabenau H, Panning M, Kolesnikova L, Fouchier RA, Berger A, Burguiere AM, Cinatl J, Eickmann M, Escriou N, Grywna K, Kramme S, Manuguerra JC, Muller S, Rickerts V, Sturmer M, Vieth S, Klenk HD, Osterhaus AD, Schmitz H, Doerr HW.** 2003. Identification of a novel coronavirus in patients with severe acute respiratory syndrome. N Engl J Med **348:**1967–1976.
11. **Fouchier RA, Kuiken T, Schutten M, van Amerongen G, van Doornum GJ, van den Hoogen BG, Peiris M, Lim W, Stohr K, Osterhaus AD.** 2003. Aetiology: Koch's postulates fulfilled for SARS virus. Nature **423:**240.
12. **Hamming I, Timens W, Bulthuis ML, Lely AT, Navis GJ, van Goor H.** 2004. Tissue distribution of ACE2 protein, the functional receptor for SARS coronavirus. A first step in understanding SARS pathogenesis. J Pathol **203:**631–637.
13. **Hwang DM, Chamberlain DW, Poutanen SM, Low DE, Asa SL, Butany J.** 2005. Pulmonary pathology of severe acute respiratory syndrome in Toronto. Mod Pathol **18:**1–10.
14. **Imai Y, Kuba K, Rao S, Huan Y, Guo F, Guan B, Yang P, Sarao R, Wada T, Leong-Poi H, Crackower MA, Fukamizu A, Hui CC, Hein L, Uhlig S, Slutsky AS, Jiang C, Penninger JM.** 2005. Angiotensin-converting enzyme 2 protects from severe acute lung failure. Nature **436:**112–116.
15. **Ksiazek TG, Erdman D, Goldsmith CS, Zaki SR, Peret T, Emery S, Tong S, Urbani C, Comer JA, Lim W, Rollin PE, Dowell SF, Ling AE, Humphrey CD, Shieh WJ, Guarner J, Paddock CD, Rota P, Fields B, DeRisi J, Yang JY, Cox N, Hughes JM, LeDuc JW, Bellini WJ, Anderson LJ; SARS Working Group.** 2003. A novel coronavirus associated with severe acute respiratory syndrome. N Engl J Med **348:**1953–1966.
16. **Kuba K, Imai Y, Rao S, Gao H, Guo F, Guan B, Huan Y, Yang P, Zhang Y, Deng W, Bao L, Zhang B, Liu G, Wang Z, Chappell M, Liu Y, Zheng D, Leibbrandt A, Wada T, Slutsky AS, Liu D, Qin C, Jiang C, Penninger JM.** 2005. A crucial role of angiotensin converting enzyme 2 (ACE2) in SARS coronavirus-induced lung injury. Nat Med **11:**875–879.
17. **Kuiken T, Fouchier RA, Schutten M, Rimmelzwaan GF, van Amerongen G, van Riel D, Laman JD, de Jong T, van Doornum G, Lim W, Ling AE, Chan PK, Tam JS, Zambon MC, Gopal R, Drosten C, van der Werf S, Escriou N, Manuguerra JC, Stohr K, Peiris JS, Osterhaus AD.** 2003. Newly discovered coronavirus as the primary cause of severe acute respiratory syndrome. Lancet **362:**263–270.
18. **Lang ZW, Zhang LJ, Zhang SJ, Meng X, Li JQ, Song CZ, Sun L, Zhou YS, Dwyer DE.** 2003. A clinicopathological study of three cases of severe acute respiratory syndrome (SARS). Pathology **35:**526–531.
19. **Lawler JV, Endy TP, Hensley LE, Garrison A, Fritz EA, Lesar M, Baric RS, Kulesh DA, Norwood DA, Wasieloski LP, Ulrich MP, Slezak TR, Vitalis E, Huggins JW, Jahrling PB, Paragas J.** 2006. Cynomolgus macaque as an animal model for severe acute respiratory syndrome. PLoS Med **3:**e149.
20. **Li W, Moore MJ, Vasilieva N, Sui J, Wong SK, Berne MA, Somasundaran M, Sullivan JL, Luzuriaga K, Greenough TC, Choe H, Farzan M.** 2003. Angiotensin-converting enzyme 2 is a functional receptor for the SARS coronavirus. Nature **426:**450–454.
21. **Liu S, Xiao G, Chen Y, He Y, Niu J, Escalante CR, Xiong H, Farmar J, Debnath AK, Tien P, Jiang S.** 2004. Interaction between heptad repeat 1 and 2 regions in spike protein of SARS-associated coronavirus: implications for virus fusogenic mechanism and identification of fusion inhibitors. Lancet **363:**938–947.
22. **Marra MA, Jones SJ, Astell CR, Holt RA, Brooks-Wilson A, Butterfield YS, Khattra J, Asano JK, Barber SA, Chan SY, Cloutier A, Coughlin SM, Freeman D, Girn N, Griffith OL, Leach SR, Mayo M, McDonald H, Montgomery SB, Pandoh PK, Petrescu AS, Robertson AG, Schein JE, Siddiqui A, Smailus DE, Stott JM, Yang GS, Plummer F, Andonov A, Artsob H, Bastien N, Bernard K, Booth TF, Bowness D, Czub M, Drebot M, Fernando L, Flick R, Garbutt M, Gray M, Grolla A, Jones S, Feldmann H, Meyers A, Kabani A, Li Y, Normand S, Stroher U, Tipples GA, Tyler S, Vogrig R, Ward D, Watson B, Brunham RC, Krajden M, Petric M, Skowronski DM, Upton C, Roper RL.** 2003. The genome sequence of the SARS-associated coronavirus. Science **300:**1399–1404.
23. **Martina BE, Haagmans BL, Kuiken T, Fouchier RA, Rimmelzwaan GF, Van Amerongen G, Peiris JS, Lim W, Osterhaus AD.** 2003. Virology: SARS virus infection of cats and ferrets. Nature **425:**915.
24. **McCray PB Jr, Pewe L, Wohlford-Lenane C, Hickey M, Manzel L, Shi L, Netland J, Jia HP, Halabi C, Sigmund CD, Meyerholz DK, Kirby P, Look DC, Perlman S.** 2007. Lethal infection in K18-hACE2 mice infected with SARS-CoV. J Virol **81:**813–821.
25. **Oudit GY, Crackower MA, Backx PH, Penninger JM.** 2003. The role of ACE2 in cardiovascular physiology. Trends Cardiovasc Med **13:**93–101.
26. **Qin C, Wang J, Wei Q, She M, Marasco WA, Jiang H, Tu X, Zhu H, Ren L, Gao H, Guo L, Huang L, Yang R, Cong Z, Guo L, Wang Y, Liu Y, Sun Y, Duan S, Qu J, Chen L, Tong W, Ruan L, Liu P, Zhang H, Zhang J, Zhang H, Liu D, Liu Q, Hong T, He W.** 2005. An animal model of SARS produced by infection of *Macaca mulatta* with SARS coronavirus. J Pathol **206:**251–259.
27. **Roberts A, Paddock C, Vogel L, Butler E, Zaki S, Subbarao K.** 2005. Aged BALB/c mice as a model for increased severity of severe acute respiratory syndrome in elderly humans. J Virol **79:**5833–5838.
28. **Roberts A, Vogel L, Guarner J, Hayes N, Murphy B, Zaki S, Subbarao K.** 2005. Severe acute respiratory syndrome coronavirus infection of golden Syrian hamsters. J Virol **79:**503–511.
29. **Rowe T, Gao G, Hogan RJ, Crystal RG, Voss TG, Grant RL, Bell P, Kobinger GP, Wivel NA, Wilson JM.** 2004. Macaque model for severe acute respiratory syndrome. J Virol **78:**11401–11404.
30. **Schlagenhauf P, Ashraf H.** 2003. Severe acute respiratory syndrome spreads worldwide. Lancet **361:**1017.
31. **Simmons G, Reeves JD, Rennekamp AJ, Amberg SM, Piefer AJ, Bates P.** 2004. Characterization of severe acute respiratory syndrome-associated coronavirus (SARS-CoV) spike glycoprotein-mediated viral entry. Proc Natl Acad Sci U S A **101:**4240–4245.

32. **Tipnis SR, Hooper NM, Hyde R, Karran E, Christie G, Turner AJ.** 2000. A human homolog of angiotensin-converting enzyme: cloning and functional expression as a captopril-insensitive carboxypeptidase. J Biol Chem **275:**33238–33243.
33. **Tsang KW, Ho PL, Ooi GC, Yee WK, Wang T, Chan-Yeung M, Lam WK, Seto WH, Yam LY, Cheung TM, Wong PC, Lam B, Ip MS, Chan J, Yuen KY, Lai KN.** 2003. A cluster of cases of severe acute respiratory syndrome in Hong Kong. N Engl J Med **348:**1977–1985.
34. **Tseng CT, Huang C, Newman P, Wang N, Narayanan K, Watts DM, Makino S, Packard M, Zaki SR, Chan TS, Peters CJ.** 2007. SARS coronavirus infection of mice transgenic for the human angiotensin-converting enzyme 2 (hACE2) virus receptor. J Virol **81:**1162–1173.
35. **Wang P, Chen J, Zheng A, Nie Y, Shi X, Wang W, Wang G, Luo M, Liu H, Tan L, Song X, Wang Z, Yin X, Qu X, Wang X, Qing T, Ding M, Deng H.** 2004. Expression cloning of functional receptor used by SARS coronavirus. Biochem Biophys Res Commun **315:**439–444.
36. **Xiao X, Chakraborti S, Dimitrov AS, Gramatikoff K, Dimitrov DS.** 2003. The SARS-CoV S glycoprotein: expression and functional characterization. Biochem Biophys Res Commun **312:**1159–1164.
37. **Yagil Y, Yagil C.** 2003. Hypothesis: ACE2 modulates blood pressure in the mammalian organism. Hypertension **41:**871–873.
38. **Zhao Z, Zhang F, Xu M, Huang K, Zhong W, Cai W, Yin Z, Huang S, Deng Z, Wei M, Xiong J, Hawkey PM.** 2003. Description and clinical treatment of an early outbreak of severe acute respiratory syndrome (SARS) in Guangzhou, PR China. J Med Microbiol **52:**715–720.
39. **Zhong NS, Zheng BJ, Li YM, Poon, Xie ZH, Chan KH, Li PH, Tan SY, Chang Q, Xie JP, Liu XQ, Xu J, Li DX, Yuen KY, Peiris, Guan Y.** 2003. Epidemiology and cause of severe acute respiratory syndrome (SARS) in Guangdong, People's Republic of China, in February 2003. Lancet **362:**1353–1358.